SUPPLEMENTARY INFORMATION

Inhaled Carbon Nanotubes Reach the Sub-Pleural Tissue in Mice

Jessica P. Ryman-Rasmussen[1,4], Mark F. Cesta[1,4,5], Arnold R. Brody[2], Jeanette K. Shipley-Phillips[3], Jeffrey Everitt[3], Earl W. Tewksbury[4], Owen R. Moss[4], Brian A. Wong[4], Darol E. Dodd[4], Melvin E. Andersen[4], and James C. Bonner[1]

[1]Department of Environmental and Molecular Toxicology, College of Agricultural and Life Sciences, North Carolina State University Raleigh, North Carolina, 27695, USA

[2]Department of Molecular Biomedical Sciences, North Carolina State University, Raleigh, North Carolina, 27695, USA

[3]Department of Population Health and Pathobiology, College of Veterinary Medicine, North Carolina State University, Raleigh, North Carolina, 27695, USA

[4]The Hamner Institutes for Health Sciences, Research Triangle Park, North Carolina, 27709, USA

[5]Laboratory of Experimental Pathology, National Institute of Environmental Health Sciences, Research Triangle Park, North Carolina, 27709, USA

The Supplementary Information contains the following: Supplementary methods, data and figures.

Supplementary Methods

MWCNT aerosol generation and characterization. Physico-chemical characteristics of the MWCNT used in this study are shown in **Table S1** and have been previously described (see reference #3 in main text). Aerosols of MWCNT suspensions and the DPBS/0.1% pluronic F-68 vehicle were generated with a 6-Jet Collision nebulizer (Model CN-25, BGI Inc, Waltham, MA) with compressed, hepa-filtered air (approximately 21psi) used as the carrier gas. **Fig. S1** and **Fig. S2** show a schematic illustration and photograph of the inhalation setup, respectively. Nebulized aerosols were passed through a trap (Model F73G-3AN-QT3, Norgren, Littleton, CO) to remove any large droplets, followed by a ^{85}Kr source (BGI-085, 10 mCi nomial, Isotope Products, Valencia, CA) and a silica gel dryer (Model 3062, TSI Inc., St. Paul, MN) to remove water. Ten animals were exposed to the aerosols on a Cannon nose-only tower (Lab Products, Maywood, NJ) for a 6 hour period at a flow rate of approximately 217 ml/min per port. The pressure at the tower was monitored with a Magnehelic pressure gauge (Magnehelic, Dywer Instruments Inc.) and maintained near 0.0 inches of water. An Aerodynamic Particle Sizer (APS, Model 3321, TSI Inc., St. Paul, MN) and a Scanning Mobility Particle Sizer (SMPS, Model 3936, TSI Inc., St. Paul, MN) were used to monitor the particle size at the inlet of the tower during each exposure. Data merge software (Model390069, TSI Inc., St Paul, MN) was used to combine APS and SMPS size distributions. Samples of the MWCNT aerosol for TEM analysis were captured from a tower port using an electrostatic precipitator (ESP, Intox Products, Moriarty, NM). Aerosol mass concentration was determined gravimetrically for each exposure at a tower port using 25 mm glass fiber filters (G15WP02500, Osmonics Inc., Minnetonka, MN). Mass mean aerodynamic diameter (MMAD) values are shown for MWCNT and CB (**Fig. S3**).

Image analysis for quantifying pleural mononuclear cell aggregates. The method for quantifying mononuclear cell aggregates was essentially the same as reported by Poland *et al*. for measuring pleural lesions on the diaphragm (ref. 2 main text). Digital images of pleural mononuclear cell aggregates from hematoxylin and eosin-stained serial sections of left lung were taken at 100X final magnification (10X original magnification x 10X eyepiece) using an Olympus BX41 light microscope with an Olympus DP71 digital camera and capture software (Olympus America, Inc, Center Valley, PA). Low magnification images of mouse lung (40X final magnification) were re-aligned using Adobe Photoshop CS3 (Adobe System, Inc., San Jose, CA) to reconstruct the entire lung section in order to measure the total pleural perimeter of that section (**Fig. S4**). The total lung perimeter was measured using Adobe Photoshop CS3 by calibrating the measurement scale tool to convert pixels into mm and then using the lasso tool to trace the perimeter of the pleural surface. Pleural mononuclear cell aggregates were then measured in an identical fashion to derive mononuclear cell aggregate perimeter (mm) and area (in mm^2). The area of a mononuclear cell aggregate was then related to the total pleural perimeter of an entire lung section as shown in **Fig. S4** and expressed as mm^2/mm. Results from a minimum of 5 separate animals for each treatment were analyzed using one way analysis of variance (ANOVA) with a Dunnett's multiple comparison post test. The data are shown in Fig. 2D.

Point counting method for estimating sizes of pleural mononuclear cell aggregates and pleural fibrotic lesions. Semi-quantitative analysis of pleural mononuclear cell aggregates and pleural fibrotic lesions was performed using a modification of the method described by Ogami *et al* (ref. 14 main text). Digital images of pleural mononuclear cell aggregates from hematoxylin and eosin-stained serial sections of left lung were taken at 100X final

magnification (10X original magnification x 10X eyepiece) using an Olympus BX41 light microscope with an Olympus DP71 digital camera (Olympus America, Inc, Center Valley, PA). A 300-point grid (20 x 15) was placed over each image on the computer screen and the percentage of tissue intersects with points was evaluated. A ‘pleural score’ was defined as the number of points that intersected the mononuclear cell aggregates divided by the total number of points covering lung tissue, including alveolar spaces. A ‘parenchymal score’ was defined as the number of points that intersected alveolar walls divided by the total number of points covering lung tissue. The ‘pleural mononuclear cell aggregate index’ was defined as the pleural/parenchymal score ratio. The point counting method to quantify pleural mononuclear cell aggregates yielded essentially the same results as the image analysis method shown in **Fig. 3d**. A comparison of the data generated by both methods is shown in **Fig. S5**.

To evaluate the extent of fibrosis, digital images were taken from Masson’s trichrome stained lung sections. A representative digital image of minimal collagen thickness and a representative digital image of maximal collagen thickness were taken from each lung at 400X final magnification (40X original magnification x 10X eyepiece). A 300-point grid was placed over each image on the computer screen and the percentage of tissue intersects with points was evaluated. Pleural and parenchymal scores were calculated as described above and a ‘fibrosis score’ was derived by taking the pleural/parenchymal ratio and averaging two images: a representative area of minimal pleural collagen thickness and a representative area of maximal collagen thickness. Representative images of minimal and maximal pleural collagen thickness were evaluated by the point-counting method (**Fig. S6**).

Supplementary Table 1. Comparison of physicochemical characterization of bulk multi-walled carbon nanotubes by the manufacturer and an independent contract laboratory. ND: not determined.

Characteristic		**Manufacturer (Helix)**	**Independent (MRL)**
Purity	**(TGA)**	**>95%**	**>94%**
Amorphous Carbon	**(TGA)**	**<2%**	**ND**
Ash	**(TGA)**	**<0.2 wt %**	**ND**
C	**(EDX)**	**93.4%**	**93.75 ± 3.93 %**
O	**(EDX)**	**6.4%**	**0.71 ± 0.19 %**
Ni	**(EDX)**	**0.12%**	**5.53 ± 3.92%**
La	**(EDX)**	**0.06%**	**ND**
C	**(ICP-AES)**	**ND**	**99.00%**
O	**(ICP-AES)**	**ND**	**0.63%**
Ni	**(ICP-AES)**	**ND**	**0.34%**
La	**(ICP-AES)**	**ND**	**0.03%**
Avg. Diameter	**(TEM)**	**10-30 nm**	**30-50 nm**
Length	**(TEM, SEM)**	**0.5-40 µm**	**0.3-50 µm**
Surface Area	**(BET)**	**40-300 m^2/g**	**109.29 m^2/g**

Definition of abbreviations: BET, Brunauer-Emmett-Teller method; EDX, energy dispersive X-ray analysis; ICP-AES, inductively coupled plasma Auger electron spectroscopy; MRL, Millennium Research Laboratories, Inc.; ND, not determined; SEM, scanning electron microscopy; TEM, transmission electron microscopy; TGA, thermogravimetric analysis.

Supplementary Table 2. Incidence of pleural mononuclear cell aggregates in mice after inhalation of multi-walled carbon nanotubes (MWCNT) or carbon black (CB) nanoparticles. The data represent the number of animals with pleural mononuclear cell aggregates/total number of animals. Note that incidence is highest for MWCNT-HI at 1 day and that this resolves to control levels by 6 weeks. The number of aggregates per 10 serial lung sections and size of aggregates is shown within the main text in **Fig. 3c** and **3d**, respectively.

	1 dy	**2 wk.**	**6 wk.**	**14 wk.**
Control	2/10	3/10	4/10	4/10
CB	3/10	4/10	3/10	5/10
MWCNT-HI	8/10	7/10	5/10	5/10
MWCNT-LO	4/10	4/10	5/10	2/10

Supplementary Table 3. Incidence of subpleural fibrosis in mice after inhalation of multi-walled carbon nanotubes (MWCNT) or carbon black (CB) nanoparticles. The data represent the number of animals with subpleural fibrosis/total number of animals. Note that incidence is highest for MWCNT-HI at 2 weeks and that this resolves to control levels by 14 weeks. Quantitative measurement of subpleural collagen thickness in fibrotic lesions is shown in **Fig. 4c**.

	1 dy	**2 wk.**	**6 wk.**	**14 wk.**
Control	0/10	0/10	0/10	0/10
CB	0/10	2/10	1/10	0/10
MWCNT-HI	0/10	9/10	6/10	1/10
MWCNT-LO	0/10	1/10	1/10	3/10

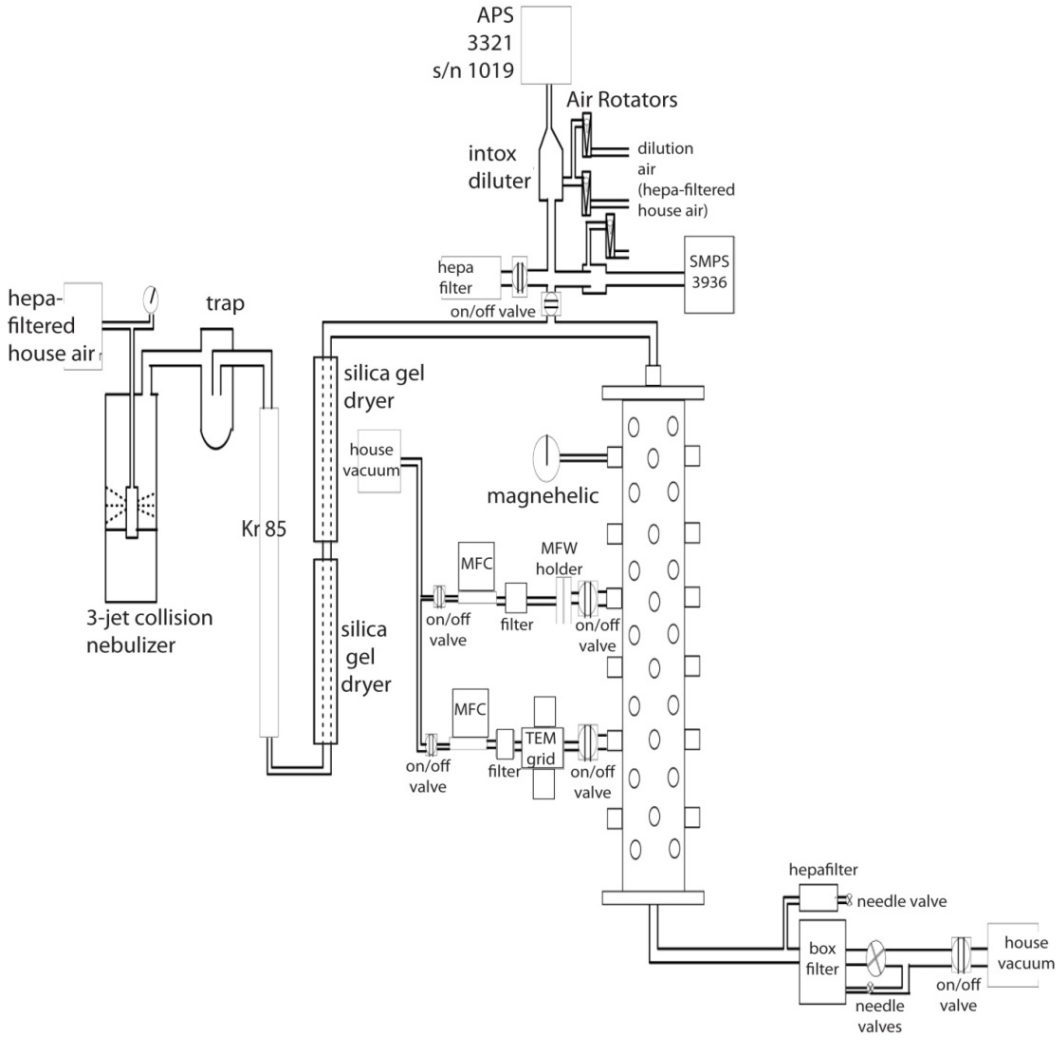

Supplementary Fig. 1. **Schematic for inhalation setup for exposure of mice to MWCNT**. Dispersion of MWCNT is achieved in the collision nebulizer at far left. MWCNT aerosol is passed through a trap to remove large droplets and Kr-85 source and silica gel to remove water. The position of an Aerodynamic Particle Sizer (APS 3321) and a Scanning Mobility Particle Sizer (SMPS 3936) are indicated. Aerosolized MWCNT enter a top port in the Cannon tower where mice receive a nose-only dose. Tower pressure is monitored via a Magnehelic pressure guage. Grids positioned distal to the central Tower collect MWCNT samples for TEM or SEM.

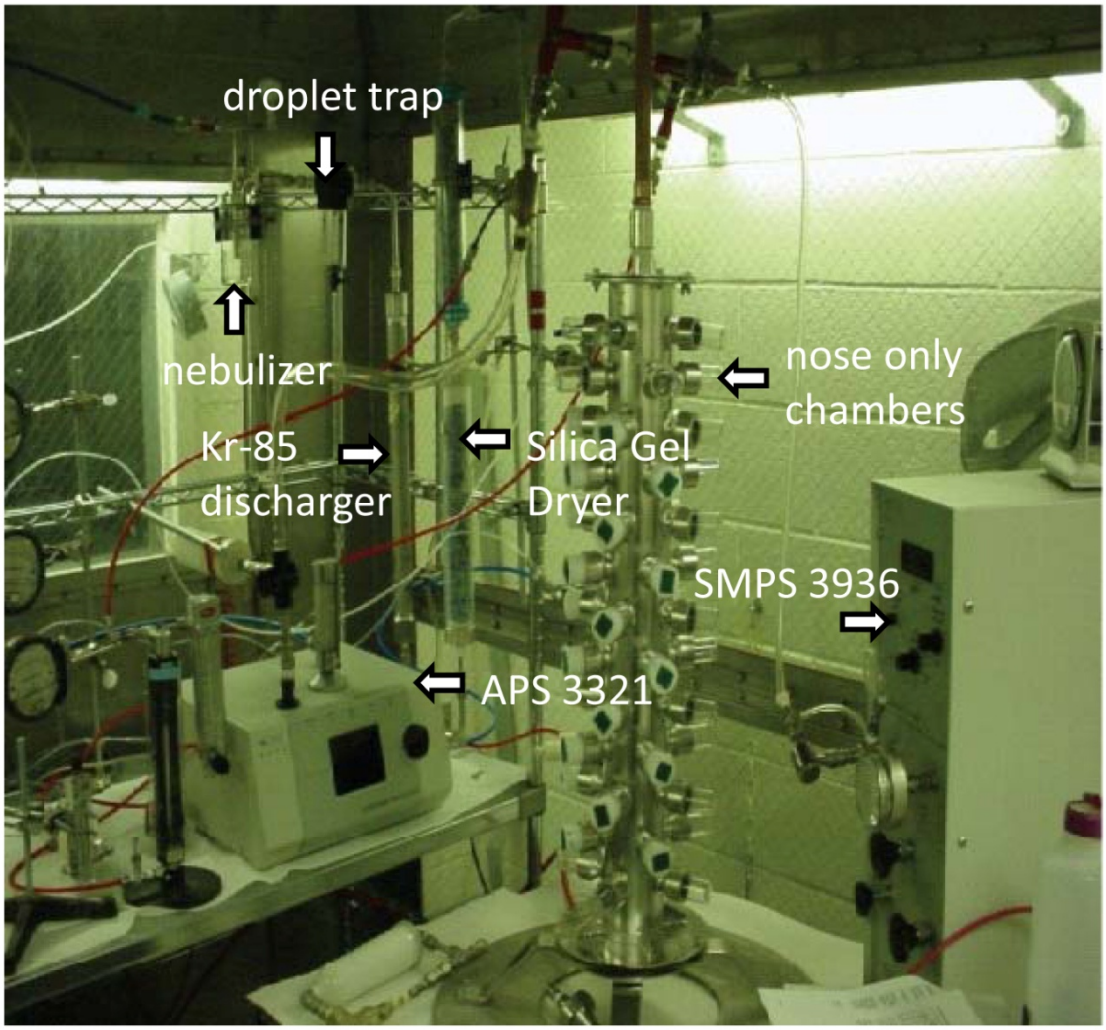

Supplementary Fig. 2. **Photograph of the inhalation setup for exposure of mice to MWCNT that is illustrated in Fig. S1**. Dispersion of MWCNT is achieved in the collision nebulizer at far left. MWCNT aerosol is passed through a trap to remove large droplets and Kr-85 source and silica gel to remove water. The position of an Aerodynamic Particle Sizer (APS 3321) and a Scanning Mobility Particle Sizer (SMPS 3934) are indicated.

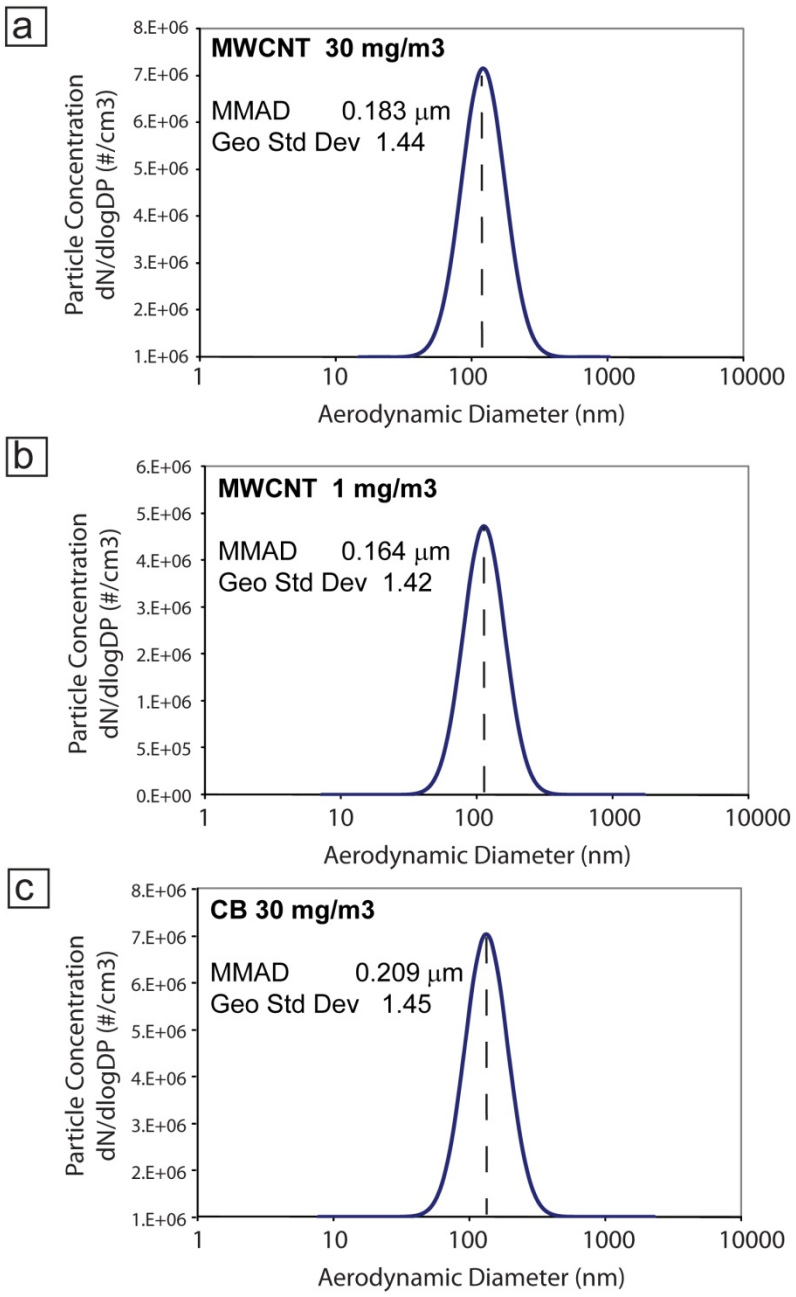

Supplementary Figure 3. **Size distribution of nanoparticle agglomerates generated by the aerosolization apparatus**. **a**, High concentration MWCNT exposure (30 mg/m^3). **b**, Low concentration MWCNT exposure (1 mg/m^3). **c**, Carbon black (CB) nanoparticle exposure (30 mg/m^3). Values shown are mass median aerodynamic diameter (MMAD) along with geometric standard deviation (Geo Std Dev).

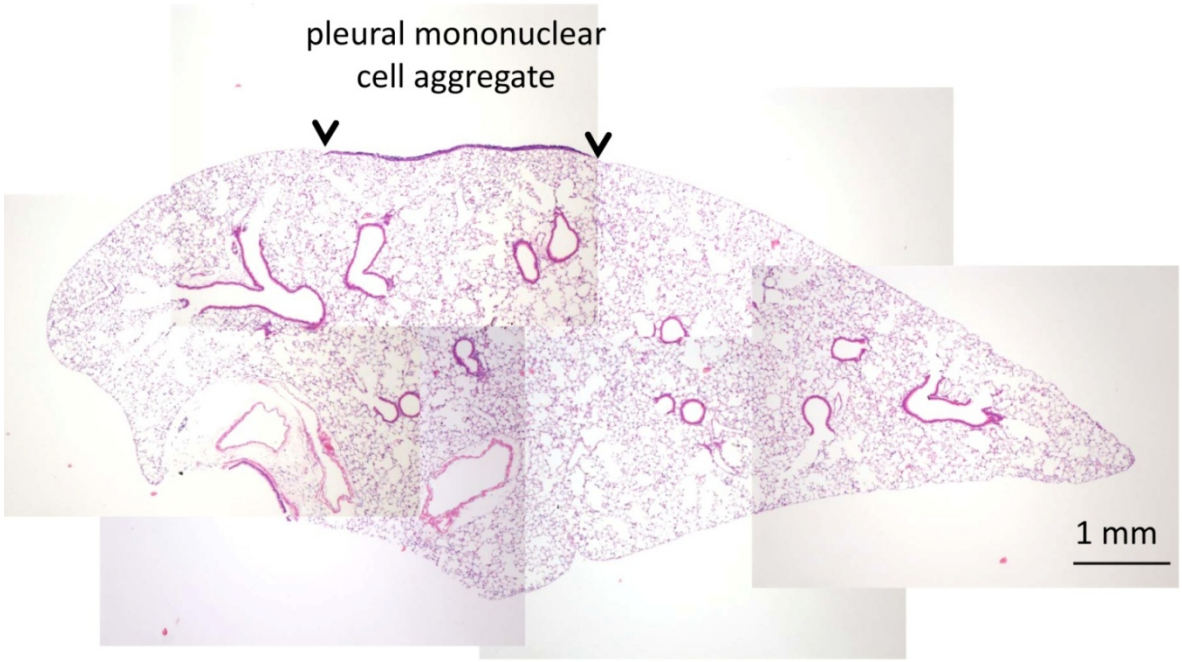

Supplementary Fig. 4. **Relationship of a pleural mononuclear cell aggregate to the total lung perimeter in a representative section**. Images of mouse lung (40X) were re-aligned using Adobe Photoshop to reconstruct the entire lung section in order to measure the total pleural perimeter of that section. The total lung perimeter was measured using Adobe Photoshop CS3 by calibrating the measurement scale tool to convert pixels into mm and then using the lasso tool to trace the perimeter of the pleural surface. Pleural mononuclear cell aggregates were measured in an identical fashion to derive mononuclear cell aggregate perimeter (mm) and area (in mm^2). The area of an aggregate was then related to the total pleural perimeter of an entire lung section and expressed as mm^2/mm. Results from a minimum of 5 separate animals for each treatment were analyzed using one way analysis of variance (ANOVA) with Dunnett's multiple comparison post test. The final data are shown in **Fig. 3d**.

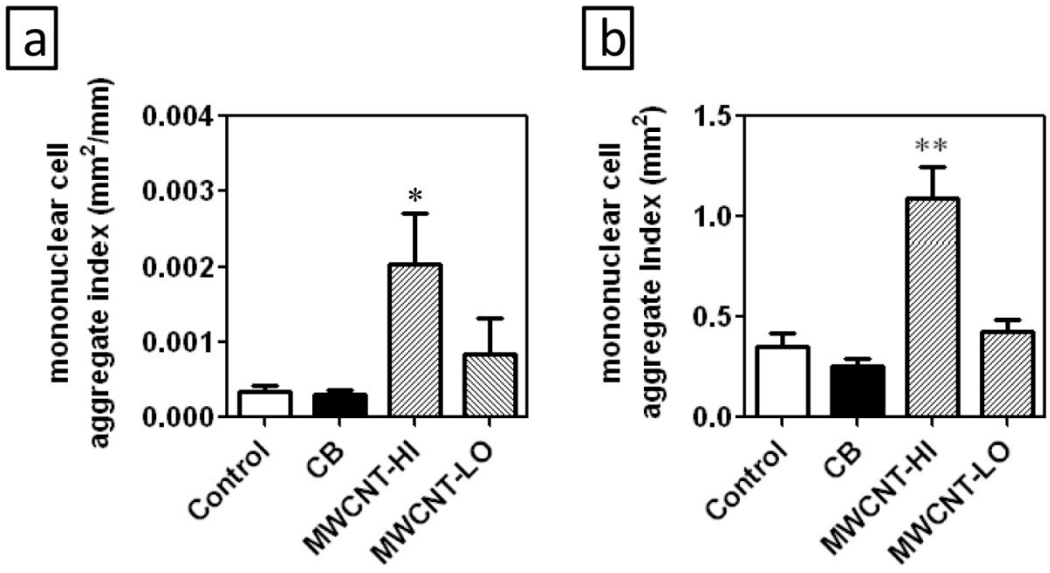

Supplementary Fig. 5. **Comparison of image analysis method using Adobe Photoshop software (a) and point counting method (b) to quantify mononuclear cell aggregate index.** The results from a minimum of 5 separate animals for each treatment were analyzed using one way analysis of variance (ANOVA) with Dunnett's multiple comparison post test. The data in panel **a** above are the same as that shown in **Fig. 3d** in the main manuscript. The point counting method yielded similar results as the image analysis method.

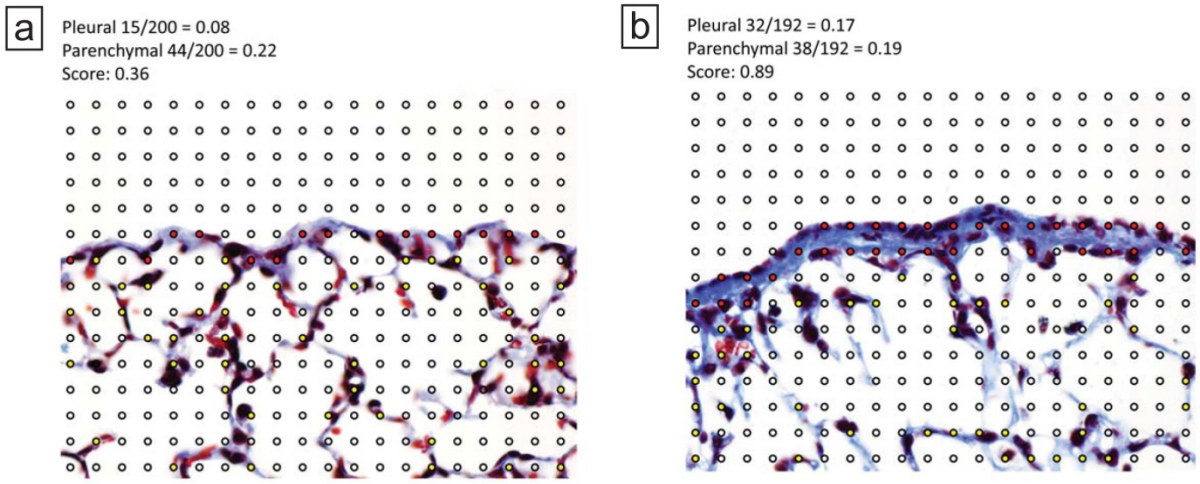

Supplementary Fig. 6. **Protocol for evaluating the extent of pleural fibrosis in mice**. Digital images were taken of lung sections stained with Masson's trichrome. Two images were captured with 400x magnification at the pleural region from each lung section; one to represent an area of minimal pleural collagen thickness (**a**) and another to represent an area of maximal collagen thickness (**b**). Data shown are from a mouse exposed to MWCNT (30 mg/m^3, 6 h) after 6 wks. The trichrome positive (blue) areas (red points) and interstitial tissue intersects (yellow points) were evaluated by the point counting method described in supplementary methods. The pleural score was calculated as number of trichrome positive points/total number of points in lung tissue and the parenchymal score as the number of tissue intersects/total number of points in lung tissue. The fibrosis score was calculated by averaging minimal and maximal pleural/parenchymal ratios for each lung.